RSS-Based Fusion of UWB and WiFi-Based Ranging for Indoor Positioning

Ghazaleh Kia[1], Jukka Talvitie[2] and Laura Ruotsalainen[3]

[1]University of Helsinki, Department of Computer Science, Helsinki, Finland
[2]Tampere University, Unit of Electrical Engineering, Tampere, Finland
[3]University of Helsinki, Department of Computer Science, Helsinki, Finland

Abstract

WiFi positioning with estimated ranges using Round Trip Time (RTT) measurements based on IEEE 802.11 Wireless Local Area Network (WLAN) has become well known since Fine Timing Measurement (FTM) protocol has been characterized. However, the multipath effect is one of the barriers to accurate time-based range measurement. On the other hand, Ultra Wide Band (UWB)-based range measurement has fair resistance to multipath effects but its accuracy is highly dependant on the orientation of the antennas in the transmitter and the receiver and its transmit power is also limited due to the applied regulations. This paper utilizes a Received Signal Strength (RSS)-based fusion of both UWB and WiFi-based range measurements to increase the indoor positioning accuracy. The proposed method takes the advantage of WiFi FTM protocol as well as Two-Way Ranging (TWR) for UWB devices. The empirical range measurement campaign is done at the University of Helsinki premises. Test points with known positions are considered as the ground truth to evaluate the results. The outcome proves that fusing UWB and WiFi ranges for indoor positioning, improves the accuracy in comparison with using the UWB or WiFi alone.

Keywords

Indoor Position Estimation, Received Signal Strength (RSS), Trilateration, UWB Two-Way Ranging (TWR), Wi-Fi Fine Timing Measurements (FTM), Wi-Fi Round-Trip Time (RTT)

1. Introduction

Signals-of-opportunity (SOOP) provide a good means for positioning indoors, where Global Navigation Satellite System (GNSS) signals are not available [1]. One of the well-known SOOP signals used for indoor positioning is WiFi [2]. There are two commonly-used methods to utilize WiFi signals for indoor positioning including RSS-based and Time-of-Flight (ToF)-based methods. The most conventional RSS-based procedure for WiFi indoor positioning is fingerprinting [3]. This method includes two phases: offline and online. In the offline phase, RSS values received from fixed anchors at each known location are collected in a data set, mapping the locations to the collected RSS values. Then, in the online phase, the online collected RSS values are compared with the previously collected RSS values in the data set and the corresponding position or an average of positions is reported as the position of the user [4]. However, acquiring the data set

IPIN 2021 WiP Proceedings, November 29 – December 2, 2021, Lloret de Mar, Spain
ghazaleh.kia@helsinki.fi (G. Kia); jukka.talvitie@tuni.fi (J. Talvitie); laura.ruotsalainen@helsinki.fi (L. Ruotsalainen)
0000-0001-7010-986X (G. Kia); 0000-0001-7685-7666 (J. Talvitie); 0000-0002-4057-4143 (L. Ruotsalainen)

is time-consuming and expensive. As another approach, WiFi can be deployed for positioning purposes by getting the RSS values to find the range between the transmitter and the receiver by signal propagation models. This method is vulnerable to variations in range measurement due to the propagation model errors [5]. To make localization easier using WiFi, IEEE released the new version of the 802.11 WLAN standard with a protocol of FTM in 2016. This protocol enables WLAN devices to find the distance between each other using RTT measurements [6]. RTT is the time it gets for a signal to travel from a user to an access point and travels back to the user after a fixed interval. RTT does not require any clock synchronization since the access point transmission is triggered by the signal of the user and the user clock offset cancels between the incoming and outgoing transmissions [4]. However, RTT is not free of problems. It provides a time-delay-based range and finding an accurate delay-based range in indoor environments with dense-multipath propagation is challenging [5]. To address the multipath effect, a general Bayesian Filter was presented in [7] to integrate RTT range measurement with map information. By this technique, authors were able to filter out the RTT-based range errors and provide a position solution with an accuracy of $3\ m$. In 2019, Dvorecki et al. in [5] have used a supervised deep learning method to estimate the RTT-based range in a dense-multipath environment. For this purpose, the authors find the first observed LOS signal path by Channel Impulse Response (CIR). Then, by having the channel estimation vector, they estimate the delay of the first observed path by Siamese Artificial Neural Network (ANN). The results prove that the ranging accuracy was increased to $4\ m$ using ANN. Another technique presented in 2019 was the use of a hybrid WiFi RTT and WiFi RSS [8]. The authors measured the ranges based on both RTT and RSS and then fused the ranges using Kalman Filter to get an accurate position solution. To evaluate their work, authors have considered a set of test points with known locations in an indoor area of $192\ m^2$. The results show that the position accuracy achieved in an indoor environment was $1.435\ m$. In 2020, the creators of WiNar have presented a combination of both RTT-based fingerprinting and ranging methods to mitigate the effects of multipath on time-based ranging. The results show that this work outperforms using RTT-based ranging or RSS-based fingerprinting alone [9]. The authors have reached an accuracy of $86\ cm$. However, in WiNar the RTT-based fingerprints should be collected and the environment-specific database should be created, which is expensive and time-consuming. Retscher et al. in [10] have presented the idea of using UWB nodes to fix the errors in WiFi RSS-based positioning. In this method, the indoor building environment is divided into different parts, and passing any UWB base stations shows that the user is in which part of the whole building. Then the results are integrated with the ranges calculated using RSS values from visible WiFi base stations and theoretical path loss models. Using this method, the authors were able to achieve $2.65\ m$ accuracy.

UWB-based positioning is a rapid developing field regarding the accuracy and the robustness it provides [11]. The accuracy in both static and dynamic positioning on reference test points are investigated in [12] and [13]. The static position investigation is done to analyze the ranging capabilities in a favorable environment. Static positioning can also be used in Wireless Sensor Network (WSN) nodes positioning, where the sensor nodes are fixed [14]. The range measurement in static condition using Pozyx devices is also addressed in [15]. The results indicate that the UWB-based range measurement can have errors as big as $1.73\ m$ and positioning can have errors more than one meter in a dense indoor environment where many

objects are causing multipath effects. This error can be increased to $5.919\ m$ when the user is dynamic in a narrow corridor [13]. Furthermore, the accuracy of UWB devices where the antenna is omnidirectional is highly dependent on the relative orientation of the transmitter and the receiver [1]. In this work, we are utilizing Pozyx developer anchors and tag, which utilize omnidirectionally radiating monopole UWB antennas [16]. However, in real positioning scenarios, it is highly probable that at some points the transmitter and the receiver directions are not heading toward each other. This can result in poor range measurement and position estimation with errors [1]. Furthermore, the ranging error of WiFi RTT tested in static positions could be as high as $1.494\ m$ even after bias removal [17]. Similarly in [18] static test points are used to evaluate the RTT-based ranging calibration. The results show that the position error in test points could be as high as $1.55\ m$. However, if the user is dynamic, using WiFi RTT for positioning is shown to have an error as high as $4\ m$ [5].

In this work, considering the UWB and WiFi RTT-based positioning, we focus on mitigating the effects of the above-discussed issues, including the limitation of transmission power and orientation-dependent accuracy of the UWB TWR, as well as multipath and position-dependent errors with the WiFi RTT. We address the error in the WiFi RTT device, present an RSS-based fusion of the UWB TWR and the WiFi RTT, and evaluate our work by using multilateration for static positions [8, 12, 13, 17, 18].

The remainder of the article is divided into the following sections. Section 2 explains the theoretical background for range measurements and multilateration. The methodology of deploying the range measurement, correcting WiFi position-dependent error, and RSS-based fusion method are presented in Section 3. Section 4 provides the experiments and results, followed by the Section 5 concluding this work.

2. Background

Radio Frequency (RF) signals are widely used for indoor positioning purposes. In this work, we address trilateration using radio-based range measurements from three anchors. Regarding the indoor environment, we investigate the two candidate signals [10]: UWB and WiFi.

2.1. WiFi RTT using FTM Protocol

Regarding the rapid use of WiFi signals in indoor positioning, FTM protocol enables an initiating device like a smartphone to find its distance to a WiFi base station like an Access Point (AP). The process begins when an initiator (it can be a mobile phone) sends an FTM request to an AP. If the AP supports the FTM process and can respond, it is called a Responder. The Responder may agree or refuse the initiator's message for the ranging procedure. If it agrees with the message, it will send an acknowledgment message (ACK) to the initiator. Then the Responder starts sending the initiator an FTM message and waits for the ACK from the initiator. The AP is allowed to send the next message only when it receives the ACK from the initiator. This procedure is illustrated in Fig. 1.

Considering the transmission timestamp of the FTM message and the reception of the ACK in the i^{th} procedure of a burst, RTT is estimated:

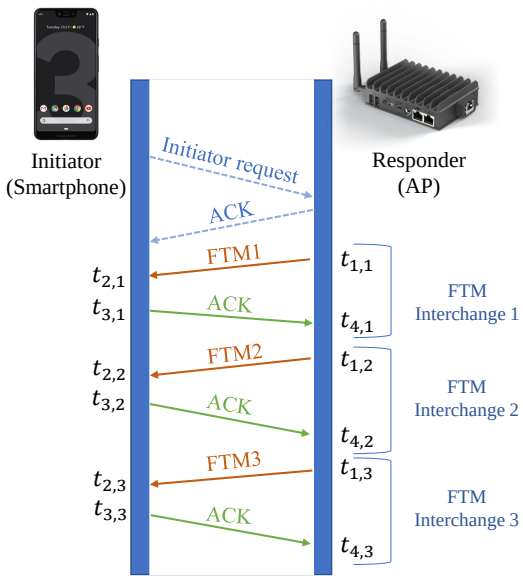

Figure 1: An overview of WiFi FTM protocol: one burst with 3 FTM exchange

$$\tau_{RTT} = (t_{4,i} - t_{1,i}) - (t_{3,i} - t_{2,i}) \tag{1}$$

where, $t_{4,i}$ is the receiving time of ACK, $t_{1,i}$ is the transmission time of the FTM message, and $t_{3,i} - t_{2,i}$ is the processing time in the mobile phone, as illustrated in Fig. 1. Several FTM-ACK processes occur in one burst. The RTT calculation continues for all the FTM-ACK processes in the burst and finally, to report the RTT, the average value will be considered.

All the timestamps are transmitted to the mobile phone to calculate the RTT. In this way, the user is enabled to estimate its position based on RTT-based ranges while its privacy is preserved [9]. The RTT shown in (1) is used to calculate the range as follows:

$$R = \frac{1}{2} \times \tau_{RTT} \times c \tag{2}$$

where c is the speed of the light. The user measures the RTT to all the responders in range, which enables the user to multilaterate its position [8]. In this work, we use trilateration to find the user position.

2.2. Trilateration

The trilateration method uses triangles geometry to estimate the target position of the mobile objects. For estimating the 2D position using multilateration, at least three base stations/anchors are required [8]. As illustrated in Fig. 2, the position of a user equipment $P = (x, y)$ can be estimated from (3) as:

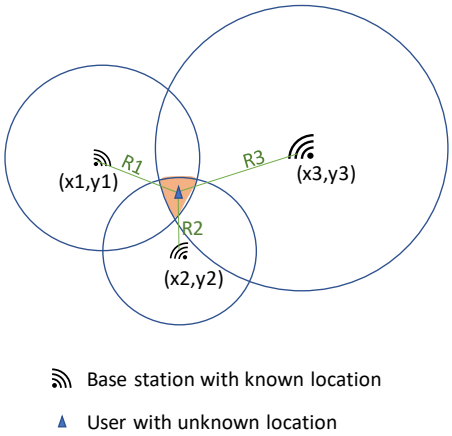

Figure 2: Positioning using anchors with known locations

$$\mathbf{P} = (\mathbf{K}^T\mathbf{K})^{-1}\mathbf{K}^T\mathbf{J} \tag{3}$$

where

$$\mathbf{K} = 2\begin{bmatrix} x_1 - x_2 & y_1 - y_2 \\ \vdots & \vdots \\ x_1 - x_n & y_1 - y_n \end{bmatrix} \tag{4}$$

and

$$\mathbf{J} = \begin{bmatrix} R_2^2 - R_1^2 - (x_2^2 - x_1^2) - (y_2^2 - y_1^2) \\ \vdots \\ R_n^2 - R_1^2 - (x_n^2 - x_1^2) - (y_n^2 - y_1^2) \end{bmatrix} \tag{5}$$

Moreover, (x_1, y_1), ..., (x_n, y_n) are the known positions of the n anchors, and $R_1, ..., R_n$ are the range measurements from the user to the n anchors.

2.3. Range Measurement using UWB TWR

UWB is a microwave signal comprising electromagnetic radiation within a frequency range from 3.1 GHz to 10.6 GHz. UWB signals are shown to propagate through walls and different materials [19]. Range measurement using UWB can be done with different techniques relying on time measurements such as Time of Arrival (ToA), Time Difference of Arrival (TDoA), and TWR. In this paper, the considered TWR approach depends on the time that RF signal requires to travel from the transmitter to the receiver, to be processed, and travel back to the transmitter. In this way, synchronization issues are conveniently solved in comparison with ToA and TDoA method, [4]. In TDoA method, the anchors are required to be accurately synchronized since the position estimation is done by finding the difference between the time stamps of the arriving

signal at the anchors [20]. By using the TWR method, the need for anchors synchronization is eliminated.

Time-based measurement can be divided into three principles including continuous-wave, impulse radio, and pseudo-noise modulation. The most commonly used method is the impulse radio. In this method, to have accurate timing a large bandwidth is required to have a narrow pulse since wide pulse results in capturing all the reflections from the environment while the signal is scattered onto the objects such as walls [12]. Regarding the fact that in UWB systems the pulse width is in order of nanosecond since the bandwidth is around 500 MHz, UWB can filter reflections of the signals to a great extent. However, the interference potential with conventional radio systems should be avoided by limiting the power spectral density. Therefore, regarding the decision of the Federal Communications Commission (FCC) in the USA and the Harmonized European Standard (EU ETSI EN 302 065), the maximum allowed isotropic radiated power density for unlicensed use of UWB is limited to $-41.3\ dBm/MHz$.

In the next section, we describe how we utilize the smartphone and the Pozyx developer tag to collect the range measurements.

3. Methodology

In this paper, we are using both UWB and WiFi anchors for obtaining the desired position estimates. To reach our goal, we have put a pair of UWB and WiFi anchors aligned on each other in three known locations, and the ranges from the user equipment to the anchors are calculated with both UWB and WiFi devices separately. The instruction of setting up the system is illustrated in Fig. 3 for the user equipment and one of the anchors.

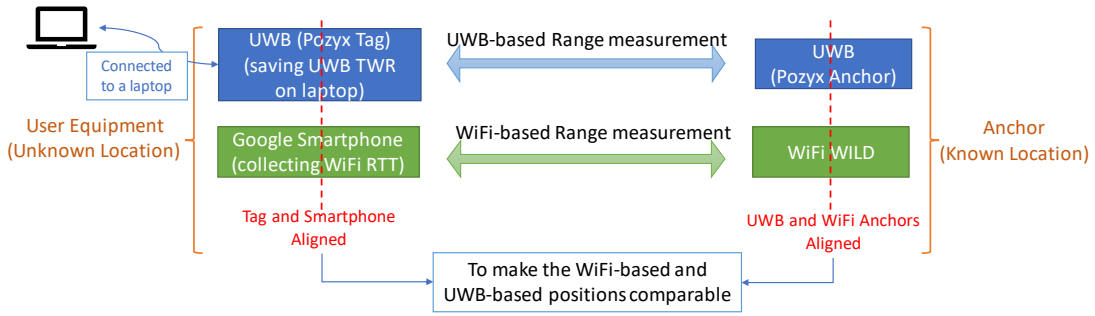

Figure 3: Instruction on setting up the system

The range measurements are collected in the reference points and averaging is used for the collected data at each point.

3.1. UWB Range Collection

To collect UWB range measurements, Pozyx developer tags are used. These tags have a Decawave DW1000 transceiver, which can operate within a frequency range from 3.5 GHz to

$6.5\ GHz$, and the power gain can be modified up to a maximum of 33 dB to control the output power. However, to assure that the signal transmitted power density stays below the maximum allowed power, the Pozyx tags average transmit power gain is set below $20\ dB$. The ranging method used for finding the distances between the Pozyx tag and the anchor is TWR. The Pozyx tag at the user equipment is connected to a laptop to save the range measurements on the laptop and get the timestamp from the operating system.

3.2. WiFi Range Collection

To collect the WiFi RTT measurements, we used a Google Pixel 3 smartphone to receive the data from WLAN anchors. This phone can support the Android RTT API as the receiver to collect the range measurements [17, 18]. The WiFi ranges and the timestamps are collected and saved in the smartphone.

3.3. WiFi Position-Dependent Error in Collected Ranges

By investigating the WiFi range measurements, we recognized that there is a non-constant error value for the measured ranges. Based on [21], there are two equipment-related issues with the WiFi devices. The first one is an offset value in the reported range measurements, which is quite repeatable and can be estimated by taking many measurements in known distances and calculating the average value. The second one is the position-dependent error in the measured ranges. To solve the latter, several measurements of the range should be done in an environment without any obstruction and find a linear fit to model the error [22]. Thus, we have done a range-measurement test inside the Anechoic Chamber of the Department of Computer Science at the University of Helsinki. The Anechoic chamber is a room that absorbs electromagnetic reflections and is isolated from interfering signals [23]. The Anechoic chamber of the department has a size of $250\ cm \times 240\ cm \times 400\ cm$ and is constructed using the Rainford EMC Systems modular panel system. The whole chamber, including the sidewalls and the ceiling, is covered with $30.5\ cm$ thick, solid, sharp-tip, resistive pyramidal foam absorbers. The chamber is shown in Fig. 4.

To do the experiment and analyze the offset and position-dependent errors, we have fixed one of the WiFi devices in the chamber and put the Google Android Phone in different distances from 0 to $200\ cm$ with $10\ cm$ increasing steps. We collected the range measurements with the Android phone for three minutes at different distances. Then we averaged the collected range measurement in each known distance to model the distances. Least-squares line fitting is used to estimate the calibrated distances based on the collected RTT-based ranges. The linear model is shown in Fig. 5, where the fitted first-order polynomial is defined as:

$$R_{calibrated} = 0.614 \times R_{collected} + 4.266 \tag{6}$$

Using this model, we were able to estimate the correct ranges with a mean error of $35\ cm$.

Figure 4: Collecting WiFi RTT measurements inside the Anechoic Chamber

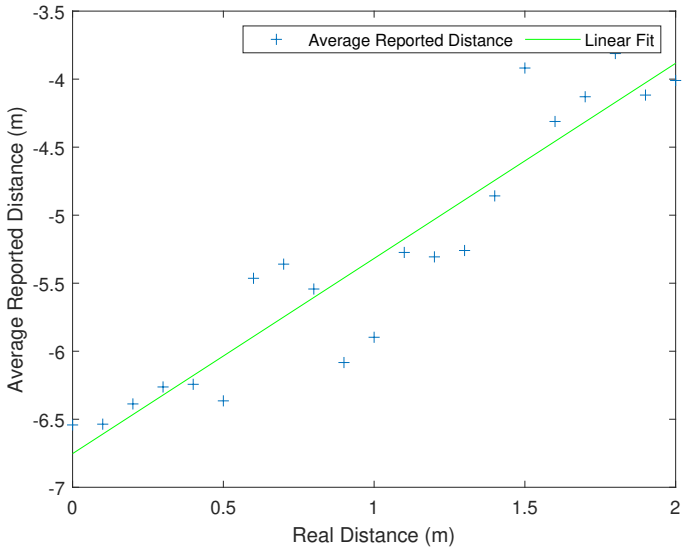

Figure 5: Use of linear fit for modeling the position-dependent error of the WiFi RTT-based range measurements

3.4. UWB and WiFi Fusion

To fuse the WiFi and UWB range measurements, we have first synchronized the smartphone and the laptop (to which the Pozyx tag is connected) by Network Time Protocol (NTP). NTP

is commonly used to synchronize the clock of network devices within the accuracy of a few milliseconds. By synchronizing the smartphone, which collects the WiFi RTT, with the laptop, which collects the UWB TWR measurements, we can fuse the measurements occurring with the same timestamp.

We take the advantage of corresponding RSS values for each range measurement. Regarding the fact that path loss and attenuation result in decreased RSS values [24], and knowing that very high RSS, in many environments indicates LOS dominated channel[5], we have defined the weights for each range measurement and calculated the weighted average of the two signals. The normalized RSS values are the parameters for defining the weights. The following equations are used to calculate the weights for fusing the measurements.

$$P_1 = \left(\frac{RSS_{UWB}}{\sum_{i=1}^{ur} RSS(i)_{UWB}}\right) \times \frac{\sigma_{UWB}^2 \times \mu_{WiFi}}{\sigma_{UWB}^2 + \sigma_{WiFi}^2} \tag{7}$$

$$P_2 = \left(\frac{RSS_{WiFi}}{\sum_{i=1}^{ur} RSS(i)_{WiFi}}\right) \times \frac{\sigma_{WiFi}^2 \times \mu_{UWB}}{\sigma_{UWB}^2 + \sigma_{WiFi}^2} \tag{8}$$

where RSS_{UWB} and RSS_{WiFi} are the corresponding RSS values for each range measurement in $watts$, ur is the update rate, $\sum_{i=1}^{ur} RSS(i)_{UWB}$ and $\sum_{i=1}^{ur} RSS(i)_{WiFi}$ are the sum of RSS values at each time epoch for UWB and WiFi, respectively.

In the definition of P_1 and P_2 the effect of RSS and accuracy are applied. In one time epoch, the number of available measurements equals the update rate of the device ur. Considering the processing of data after each time epoch while we have all the measurements occurring in one epoch, we can define the fraction $\frac{RSS}{\sum_{i=1}^{ur} RSS(i)}$ for each measurement. Larger RSS values imply a stronger signal and result in larger P_1 and P_2 values. In the second fraction of the equations (7) and (8), the effect of accuracy is applied. According to ISO 5725-1, accuracy is defined by two factors: trueness and precision, where trueness is the mean and precision is the variance of the error distribution. For applying the two factors in the RSS-based fusion, we have first found the mean and variance of the estimated position errors using UWB (μ_{UWB}, σ_{UWB}), as well as those of the estimated position errors using WiFi (μ_{WiFi}, σ_{WiFi}). Then we have defined the weights based on the mean of a Gaussian Probability Distribution Function (PDF) which is the product of the two (WiFi and UWB) Gaussian PDFs.

Finally, the weights will be calculated using (9) and (10).

$$P_{UWB} = \frac{P_1}{P_1 + P_2} \tag{9}$$

$$P_{WiFi} = \frac{P_2}{P_1 + P_2} \tag{10}$$

Thus, the final fused range value would be:

$$FusedRange = P_{WiFi} \times R_{Wifi} + P_{UWB} \times R_{UWB} \tag{11}$$

where R_{WiFi} represents the collected range measurements with WiFi devices, which are calibrated by using (6), and R_{UWB} represents the collected range with the UWB devices.

4. Experiments and Results

To test the algorithm and evaluate our work, a measurement campaign is done at the premises of the Department of Computer Science, University of Helsinki. The floor plan of the area for the test is illustrated in Fig. 6.

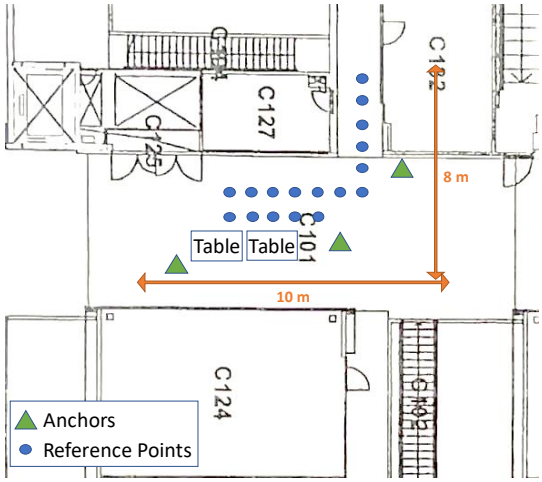

Figure 6: Floor Plan of the area of data collection

18 reference points with known locations are considered. The reference points are marked with yellow signs as illustrated in Fig. 7 and 8.

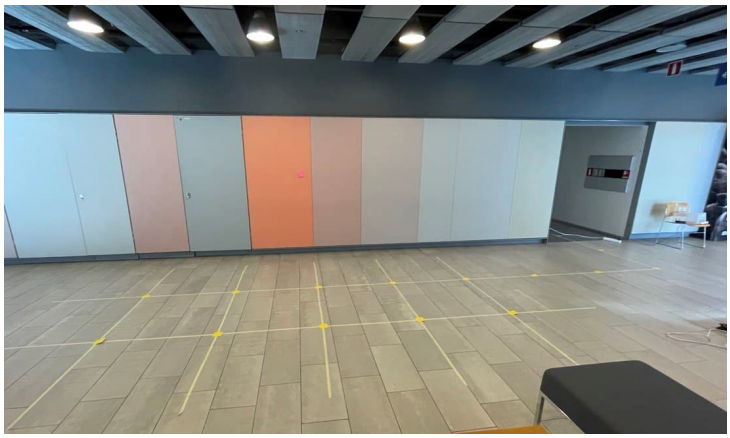

Figure 7: Reference points for evaluating the results inside the hall.

The WiFi anchors are Compulab WILD WLAN devices that are capable of providing RTT measurements. The UWB anchors are Pozyx Developer anchors. The aligned UWB and WiFi anchors in one of the base stations locations are illustrated in Fig. 9.

For the UWB modules, channel 5 is selected, preamble length is 1024, Pulse Repetition

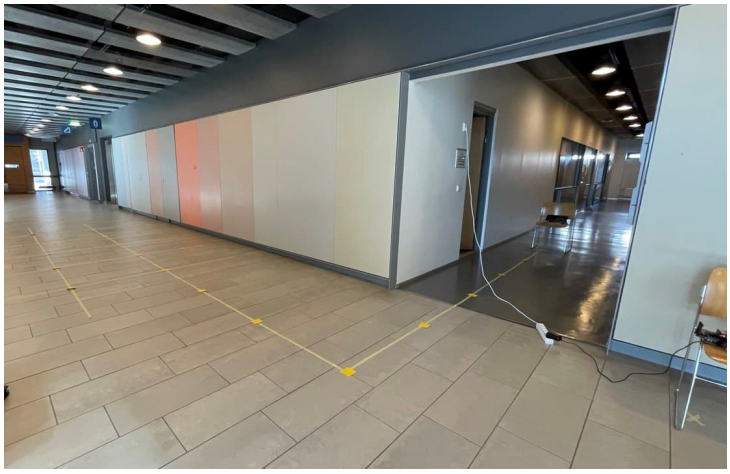

Figure 8: Reference points for evaluating the results inside the hall and the corridor.

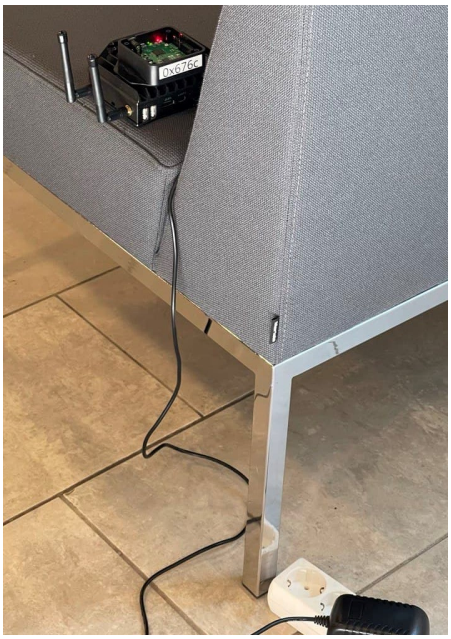

Figure 9: One of the base stations including both WiFi and UWB anchors

Frequency (PRF) is 64 MHz, bitrate is 110 $kbps$, and transmit power is 19.5 dB.

The Pozyx tag is connected to a laptop for UWB TWR collection using a developed Python code. Furthermore, the smartphone using a developed Android application is utilized for WiFi RTT collection. The phone and the tag are illustrated in Fig. 10. The range data is collected once using the synchronized smartphone and the laptop. The UWB and WiFi measurements are used both separately and fused for estimating the positions.

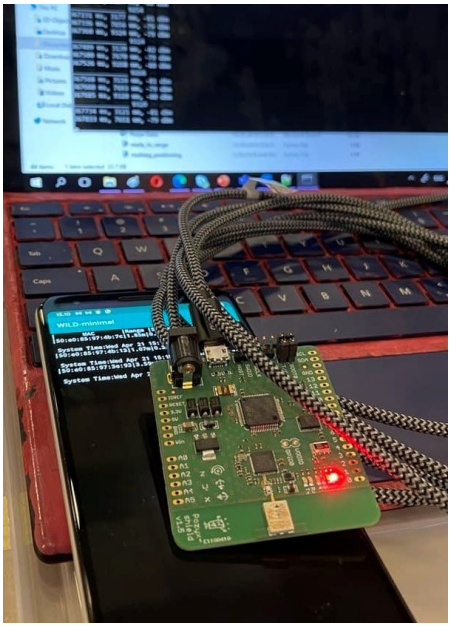

Figure 10: Pozyx tag and smart phone for data collection

4.1. WiFi-RTT based ranges for estimating the positions

Using the range measurements collected at the test points, we have first done the position estimation using WiFi-based ranges and the trilateration method. The estimated positions are illustrated in Fig. 11.

The calculated mean error of the estimated positions using only the WLAN devices is 133.9 cm.

4.2. UWB-TWR based ranges for estimating the positions

After using the WiFi-based ranges, we have used trilateration for UWB-based range measurements. The estimated positions using only UWB TWR are illustrated in Fig. 12.

Estimating the positions using only the UWB devices resulted in a mean error of 111.4 cm.

4.3. RSS-based fused range measurements for estimating the positions

After investigating the UWB and WiFi-based position estimations, we have fused the range measurements using the RSS-based algorithm presented in the methodology section. By using the fused range measurements, we were able to decrease the mean error to 75.7 cm. The estimated positions using the fused UWB and WiFi-based range measurements are illustrated in Fig. 13.

The results prove that UWB and WiFi fusion presents sub-meter level accuracy in a dense multipath indoor environment where the WiFi signals are experiencing reflections as well as position-dependent errors, and the omnidirectional antennas of Pozyx UWB devices are not

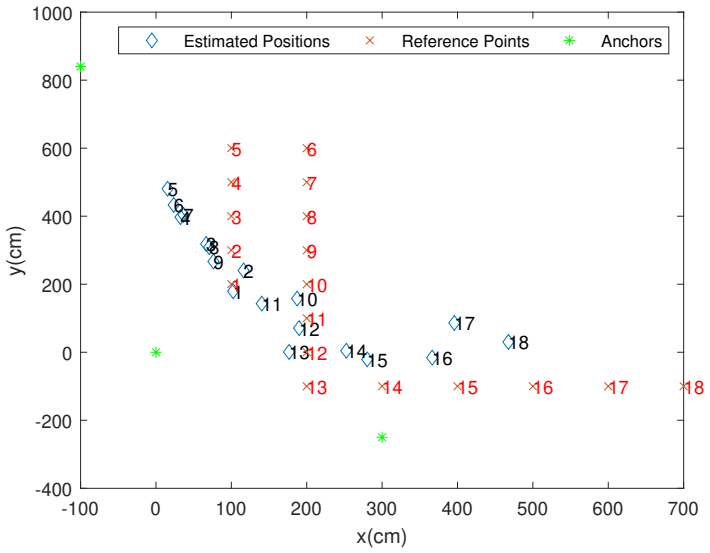

Figure 11: Estimated positions using WiFi-based range measurements

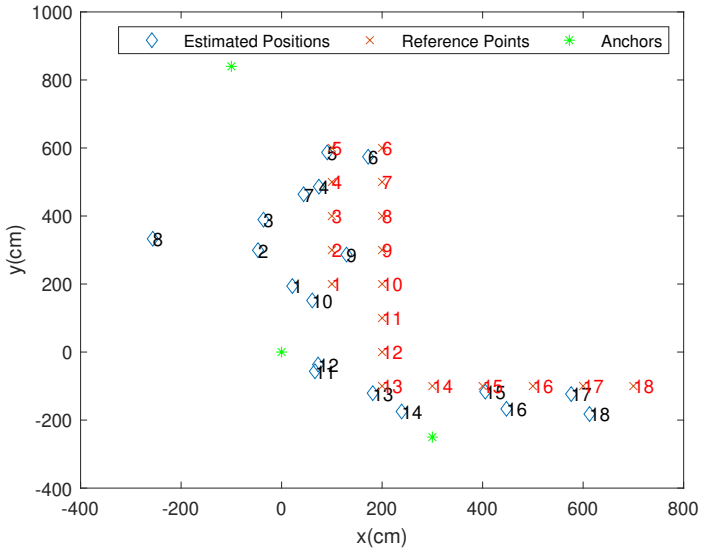

Figure 12: Estimated positions using UWB-based range measurements

necessarily heading toward each other. As summarized in Fig. 14, compared to individual UWB and WiFi-based measurements, the mean and Standard Deviation (STD) of the positioning error are decreased by $32-43\%$ and $39-51\%$, respectively, by fusing the UWB and WiFi measurements.

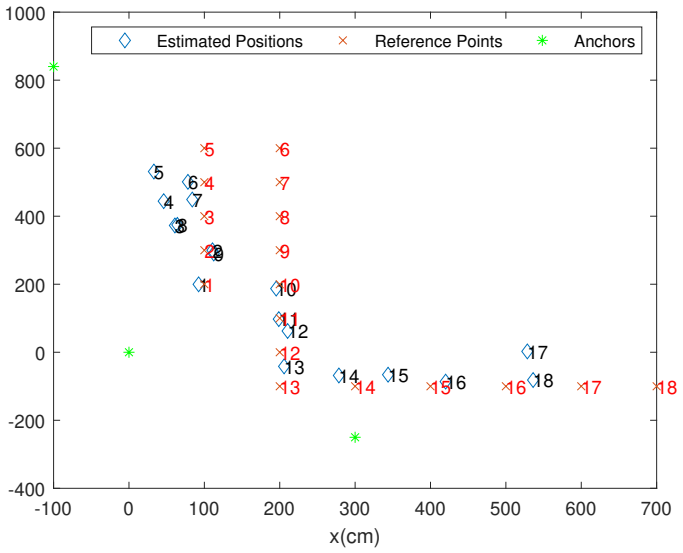

Figure 13: Estimated positions using RSS-based fused UWB and WiFi-based range measurements

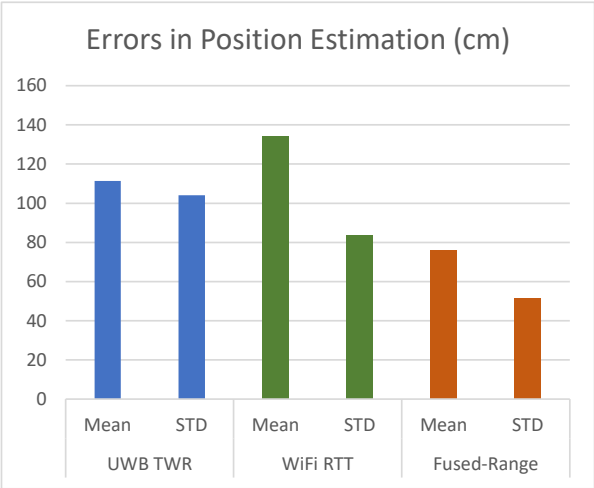

Figure 14: Errors in estimated positions using different measurements

5. Conclusion

In this work, the WiFi RTT-based ranging and UWB TWR are addressed using Compulab WLAN and Pozyx UWB devices. The range measurements are first used in the multilateration algorithm to estimate the position solution separately for the WiFi and UWB. Regarding the problem of multipath effect which is highly effective on WiFi RTT-based ranges and the problem of orientation-dependent accuracy of UWB as well as transmit power limitations by regulations,

an RSS-based fusion of the range measurements is used to investigate the superiority of the integrated ranges for the position estimation. The results confirm that the accuracy of estimated static position solutions is improved in the real indoor environment by fusing the UWB and WiFi-based range measurements. In the next steps of this research, specific noise probability distribution in the range measurements will be addressed. In addition, a mobile user with appropriate tracking algorithms is considered for a navigation application. Besides the above, it is important to investigate a larger positioning area with additional reference points for more comprehensive testing of the system behavior.

Acknowledgments

This work was funded by the European Space Agency ESA AO/2-1716/19/NL/CRS/hh and the University of Helsinki.

References

[1] P. Figueiredo E Silva, Signals of opportunity for positioning purposes, Ph.D. thesis, Tampere University of Technology, 2018. URL: http://urn.fi/URN:ISBN:978-952-15-4280-0.

[2] C. Gentner, M. Ulmschneider, I. Kuehner, A. Dammann, WiFi-RTT indoor positioning, 2020, pp. 1029–1035. doi:10.1109/PLANS46316.2020.9110232.

[3] G. Mendoza-Silva, A. C. Costa, J. Torres-Sospedra, M. Painho, J. Huerta, Environment-aware regression for indoor localization based on WiFi fingerprinting, IEEE Sensors Journal (2021) 1–1. doi:10.1109/JSEN.2021.3073878.

[4] P. Groves, Principles of GNSS, inertial, and multisensor integrated navigation systems, Second edition, 2013.

[5] N. Dvorecki, O. Bar-Shalom, L. Banin, Y. Amizur, A machine learning approach for Wi-Fi RTT ranging, 2019. doi:10.33012/2019.16702.

[6] (Revision of IEEE Std 802.11-2012) - Part 11: Wireless LAN Medium Access Control (MAC) and Physical Layer (PHY) specifications, December 7th, 2016.

[7] L. Banin, U. Schatzberg, Y. Amizur, WiFi FTM and Map information fusion for accurate positioning, in: 2016 International Conference on Indoor Positioning and Indoor Navigation (IPIN), 2016.

[8] G. Guo, R. Chen, F. Ye, X. Peng, Z. Liu, Y. Pan, Indoor Smartphone Localization: A Hybrid WiFi RTT-RSS Ranging Approach, IEEE Access 7 (2019) 176767–176781. doi:10.1109/ACCESS.2019.2957753.

[9] O. Hashem, M. Youssef, K. A. Harras, WiNar: RTT-based Sub-meter Indoor Localization using Commercial Devices, in: 2020 IEEE International Conference on Pervasive Computing and Communications (PerCom), 2020, pp. 1–10. doi:10.1109/PerCom45495.2020.9127363.

[10] G. Retscher, V. Gikas, H. Hofer, H. Perakis, A. Kealy, Range validation of UWB and Wi-Fi for integrated indoor positioning, Applied Geomatics 11 (2019). doi:10.1007/s12518-018-00252-5.

[11] M. Mäkelä, M. Kirkko-Jaakkola, J. Rantanen, L. Ruotsalainen, Proof of concept tests on cooperative tactical pedestrian indoor navigation, in: 2018 21st International Conference on Information Fusion (FUSION), 2018, pp. 1369–1376. doi:10.23919/ICIF.2018.8455380.

[12] P. Dabove, V. Di Pietra, M. Piras, A. A. Jabbar, S. A. Kazim, Indoor positioning using Ultra-wide band (UWB) technologies: Positioning accuracies and sensors' performances, in: 2018 IEEE/ION Position, Location and Navigation Symposium (PLANS), 2018. doi:10.1109/PLANS.2018.8373379.

[13] V. D. Pietra, P. Dabove, M. Piras, A. Lingua, Evaluation of positioning and ranging errors for UWB indoor applications, in: IPIN, 2019.

[14] J. Grigulo, L. B. Becker, Experimenting sensor nodes localization in WSN with UAV acting as mobile agent, in: 2018 IEEE 23rd International Conference on Emerging Technologies and Factory Automation (ETFA), volume 1, 2018, pp. 808–815. doi:10.1109/ETFA.2018.8502536.

[15] V. Di Pietra, P. Dabove, M. Piras, Loosely coupled GNSS and UWB with INS integration for indoor/outdoor pedestrian navigation, Sensors 20 (2020). doi:10.3390/s20216292.

[16] Pozyx knowledge center-Hardware setup, https://docs.pozyx.io/creator/latest/getting-started/hardware-setup/, 2021. [Online; accessed 5-May-2021].

[17] C. MA, B. Wu, S. Poslad, D. R. Selviah, Wi-Fi RTT ranging performance characterization and positioning system design, IEEE Transactions on Mobile Computing (2020) 1–1. doi:10.1109/TMC.2020.3012563.

[18] H. Cao, Y. Wang, J. Bi, S. Xu, M. Si, H. Qi, Indoor positioning method using WiFi RTT based on LOS identification and range calibration, ISPRS International Journal of Geo-Information 9 (2020). doi:10.3390/ijgi9110627.

[19] M. Mäkelä, J. Rantanen, J. Ilinca, M. Kirkko-Jaakkola, S. Kaasalainen, L. Ruotsalainen, Cooperative environment recognition utilizing uwb waveforms and cnns, in: 2020 European Navigation Conference (ENC), 2020, pp. 1–8. doi:10.23919/ENC48637.2020.9317403.

[20] W. Wang, J. Huang, S. Cai, J. Yang, Design and implementation of synchronization-free tdoa localization system based on uwb, Radioengineering 27 (2019) 320–330. doi:10.13164/re.2019.0320.

[21] B. K. P. Horn, Doubling the accuracy of indoor positioning: frequency diversity, Sensors 20 (2020) 1489. doi:10.3390/s20051489.

[22] B. K. P. Horn, Observation model for indoor positioning, Sensors 20 (2020). doi:10.3390/s20144027.

[23] Y. Wang, C. Xiu, X. Zhang, D. Yang, WiFi indoor localization with CSI fingerprinting-based random forest, Sensors 18 (2018). doi:10.3390/s18092869.

[24] F. Dümbgen, C. Oeschger, M. Kolundžija, A. Scholefield, E. Girardin, J. Leuenberger, S. Ayer, Multi-modal probabilistic indoor localization on a smartphone, in: 2019 International Conference on Indoor Positioning and Indoor Navigation (IPIN), 2019, pp. 1–8. doi:10.1109/IPIN.2019.8911765.